A FPGA-Based Multi-Frequency Current Source for Biological EIT System

Xianding Yang, Yanbin Xu, Feng Dong
Tianjin Key Laboratory of Process Measurement and Control
School of Electrical Engineering and Automation, Tianjin University
Tianjin, China
E-mail: xuyanbin@tju.edu.cn

***Abstract*—Multi-frequency electrical impedance tomography has been evolving from the frequency-sweep approach to the multi-frequency simultaneous measurement technique which can drastically reduce measuring time and will be increasingly attractive for time-varying biological applications. In order to improve the output impedance of current source and obtain more impedance information at different frequencies simultaneously, a FPGA-based multi-frequency current source is designed. New features of the proposed multi-frequency current source include feedback loop to improve the output impedance of current source, amplitude control circuit to adjust amplitude of current source and the initial phases which are considered for reducing crest factor (CF) of multisine excitation signals to obtain a further SNR improvement, compared to random phases which are used in previous design. The output performance of this current source is evaluated by simulation and actual measurement. The output impedance of current source with feedback loop is greater than the one without feedback loop. The stability of current source with feedback loop outperforms the current source without feedback loop for resistive and capacitive loads in simulation. The simulation and measurement results show that output impedance of current source significantly improves by adding feedback loop, and the multi-frequency current source can perform stably and provide high output impedance and multi-frequency simultaneously excitation signals, which is suitable for multi-frequency EIT system.**

Keywords—multi-frequency; current source; biological electrical impedance tomography; output impedance; crest factor

I. INTRODUCTION

Electrical impedance tomography (EIT) is a noninvasive, non-harmful and low-cost imaging modality to reconstruct image of the impedance distribution of a body's section by injecting small alternating currents or voltage and measuring the resulting voltages or currents on the electrodes placed on the body surface [1]. Current source and voltage source are the two kinds of signal sources used in the EIT system. However, in the voltage source circuit the input signal is needed to be adjusted according to different load down to the safety limit of the human injection current, which is relatively complicated [2]. Therefore, the current source has a wide range of applications especially in EIT [3]. In this current injection with voltage measurement phantom, the current source is an important component in electrical impedance tomography and its performance directly affects the precision of the system. Therefore, designing a high-quality excitation signal source is important to enhance the precision and signal to noise ratio (SNR) of EIT system.

Multi-frequency EIT measurement technologies are divided into the frequency-sweep (FS) approach and the multi-frequency simultaneous (MFS) measurement technique according to the different excitation mechanisms. The FS measurement technology can extract complex impedance information at different time, and it will improve the precision of typical single frequency EIT system [4]. The MFS measurement technology, which can extract full information of the impedance at the same time, drastically reduce measuring time, and grasp the transient physiological status of human body, will be increasingly attractive for time-varying biological applications [5]. Therefore, it is significant attempt to design and implement multi-frequency EIT system which extracts the real part and the imaginary part information of the impedance of biological tissue at the same time for clinical diagnosis and real-time monitoring.

In multi-frequency EIT system, the multi-frequency excitation signal source is the key component. An important parameter of multi-frequency current source is its output impedance, which is important indicator for evaluating of current source. Ideally the output impedance should be infinitely large. However, in the actual circuit design, the output impedance of current source will degrade dramatically due to the presence of stray and parasitic capacitances at higher frequencies. Thus, it is the most important and critical procedure to achieve the highest possible value of output impedance of current source in the design of current source [6]. Bandwidth of the current source is another important factor. EIT system requires a wide range of frequencies. The current source of EIT system is required to be stable over the frequency ranging 1 KHz to 1 MHz with several mA. Thus, it is very meaningful to design a current source whose amplitude and frequency can be adjusted, which has high output impedance and a wide range of frequencies and can provide both sweep frequency and multi-frequency simultaneously excitation signals in multi-frequency.

At present, many types of current source topologies have been used in EIT system, but Howland current source remains a popular choice since it can be constructed using a single operational amplifier and a handful of resistors [7]. Reference pointed out that the Howland has comparable performance to current mirror, which illustrates that both circuits are stable over the frequency range from 1 KHz to 1 MHz [8]. In order to

The authors appreciate the support from the National Natural Science Foundation of China (No. 61302122 & No. 61571321).

improve the precision and output impedance of the Howland topology current source, the generalized impedance converter (GIC) is designed in the enhanced Howland current source circuit to achieve a high precision and capacitance compensated current source for EIT application [9]. However, for the FS EIT system, the complexity of the approach is very large because for each frequency, an individual GIC needs to be applied. In a new multi-frequency EIT system called KHU Mark2.5 [10], output impedance of Howland current source with multiple GICS is up to 5.75MΩ in the frequency of 500 KHz, and the mean of the output impedance is 41.6MΩ. But the circuit of current source is very complicated. For the MFS EIT system, the current source with GIC is not suitable, because it cannot reach high output impedance and may lead to instability. A high output impedance VCCS based on the current feedback amplifier (CFA) AD844 (Analog Devices) was proposed by Bragos in 1994 [11], which has been widely adopted by many bioimpedance systems [12] including the multi-frequency simultaneous (MFS) measurement techniques [13]. In this paper, VCCS is designed according to this approach.

As for multi-frequency EIT system, there are many different types of multi-frequency excitation signals which are applied for fast impedance measurement. These excitation signals include chirp pulses, maximum length binary sequences (MLBS) and multisine excitation signals. However, the multisine signal, as the sum of a finite number of harmonically related sinusoids, has a clean spectrum and the flexibility to create arbitrary harmonic components, and is regarded as a suitable broadband excitation signal for multi-frequency EIT system. Moreover, multisine excitation with a lower crest factor (CF) (the ratio of signal peak value to its root mean square (RMS) value) can obtain a further SNR improvement [14]. A low CF multisine excitation depends on the optimum selection of the initial phases of its harmonic components. Various phase selection methods for reducing the CF of multisine excitation signals have been investigated for many years. The simplest method is to use random phases [15], but these have by far the worst CF of 3.7 [16]. A formula to choose the phases of the multisine excitation signal appropriately to control CF was firstly proposed by Schroeder, and a typical CF value could reach 1.67 for multisine excitations with equidistant and flat amplitude components [17]. In contrast to the Schroeder phases, in order to calculate the Newman phases the only the number of the exciting multisine frequencies is needed [16]. It can also have a typical CF of 1.67. It is convenient to adjust the initial phase of each frequency by changing internal parameters of DDS IP core of DDS module in the proposed FPGA-based multi-frequency current.

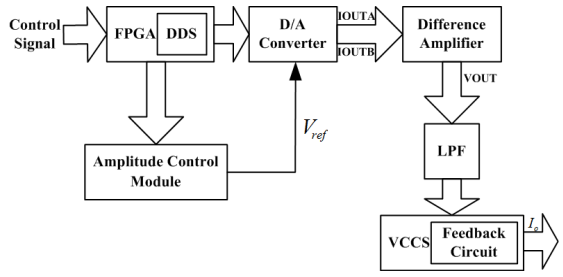

Fig. 1. Block diagram of the current source

A FPGA-based multi-frequency current source is proposed. This current source is evolved from previous design [18] in terms of technical details such as FPGA-based direct digital synthesizer module, D/A converter module, low-pass filter and voltage controlled current source. Our contribution is to specifically design the feedback loop to improve the output impedance of current source and amplitude control circuit to adjust amplitude of current source, and control initial phases which are Newman phase which have a typical CF value of 1.67, compared random phases which have a typical CF value of 3.7 in previous design to obtain a further SNR improvement. Firstly, the architecture of multi-frequency is introduced. Then, the stability, the output impedance and the loading ability of multi-frequency current source are analyzed in the simulation and measurement experiments. Finally, the design of this multi-frequency current source is summarized.

II. Design on Current Source

A. Structure of Multi-Frequency Current Source

The multi-frequency current source comprises six parts (Fig.1): (a) FPGA-based direct digital synthesizer (DDS), (b) D/A converter, (c) amplitude control module, (d) difference amplifier, (e) low-pass filter and (f) voltage controlled current source (VCCS) with feedback circuit.

In this multi-frequency current source circuit, DDS module is constructed by using hardware language in FPGA, the digital sine wave signals with the mixture of multiple frequencies are produced through FPGA, the low-pass filter is used to remove high-frequency noise, the voltage signal is converted to current by using VCCS circuit and the feedback circuit is used to improve output impedance.

B. FPGA-Based Direct Digital Synthesizer Module

DDS module is constructed by using very high speed integrated circuit hardware description language (VHDL) and DDS IP cores in FPGA, which can perform the important function of FPGA and ensure speed and reliability of the system. This DDS module can support up to 16 channels and frequencies and initial phase of each channel are controlled by the phase increment ($PINC$) and the phase offset ($POFF$). The relationships between $PINC$ and output frequency f_{out}, $POFF$ and initial phase ϕ are shown as follows

$$PINC = \frac{f_{out} \times 2^N}{f_{clk}} \tag{1}$$

$$POFF = \frac{\phi \times 2^N}{2\pi} \tag{2}$$

Where N is the number of bits of the phase accumulator.

For multisine excitation signals, multiple DDS modules can produce several different sinusoidal signals and the mixed frequency signal is obtained through adder. The initial phase of each frequency is set according to Eq. (3), which is proposed by Newman [17].

$$\phi_n = \frac{\pi n^2}{N}, n = 0,\ldots,N-1 \quad (3)$$

Where ϕ_n is initial phase and N is number of exciting multisine frequencies. The initial phase of each frequency to obtain a further SNR improvement can be controlled by changing internal parameters of DDS IP core in FPGA. So it is flexible to adjust the initial phase of each frequency in the proposed multi-frequency current source.

In this way, there is no need to change external circuit, which is also well transplanted. The multisine excitation signals are the sum of three frequencies of 100 KHz, 500 KHz and 900 KHz, and initial phases are 0, $\frac{\pi}{3}$ and $\frac{4\pi}{3}$ as shown in Fig.2.

C. D/A Converter and Amplitude Control Circuit

In the digital to analog circuit of multi-frequency current source, a 14 bit high-speed DAC is used to convert the digital sine wave signal into analog voltage signal and its update rates are up to 125 MSPs. When $f_{clk} = 50MS/s$ and $f_{out} = 1MHz$, the spurious free dynamic range (SFDR) can be up to 84dBc, effectively ensuing the DAC will not degrade the overall measurement performance.

For clinical use, the amplitude and frequency ranges of excitation signals are limited by the IEC6060-1-1 standard for patient safety and this current design assumes that the total current applied is less than 5mA [19]. Therefore, the amplitude of current source should be adjusted easily and has a large adjusting range. In this paper, the amplitude of the signal can be adjusted by using an 8 bit DAC that sets the reference voltage of the 14 bit DAC.

D. Voltage Controlled Current Source with Feedback Loop

Voltage controlled current source (VCCS) module, which can convert the voltage signal into current signal, is a core part of multi-frequency current source. Typically, VCCS circuits include the enhanced Howland circuit, single op-amp VCCS, double op-amp VCCS, three op-amp VCCS and mirror current VCCS [20]. In multi-frequency EIT system, single op-amp VCCS, double op-amp VCCS and three op-amp VCCS will lead to instability. Compared with the above VCCS circuit, the current mirror based on AD844 which is proposed by Bragos in 1994 [11] shown in Fig.3 is suitable for multi-frequency EIT system, but it cannot achieve high output impedance [8]. Therefore, there needs to be a way to improve output impedance. In this paper, the feedback loop shown in Fig.4 is specifically designed to improve output impedance.

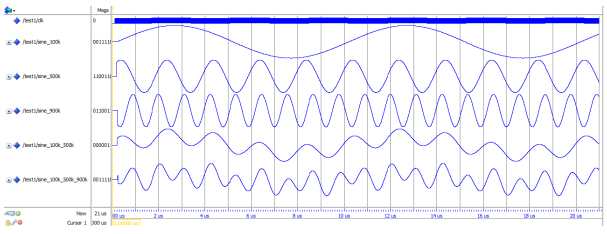

Fig. 2. Simulation waveforms of multi-frequency signal source

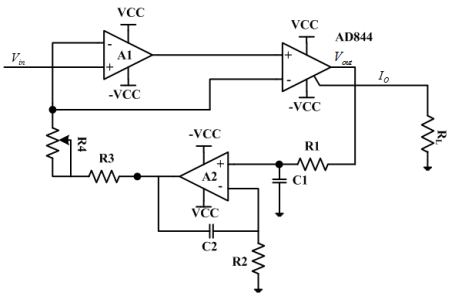

Fig. 3. Principle diagram of VCCS

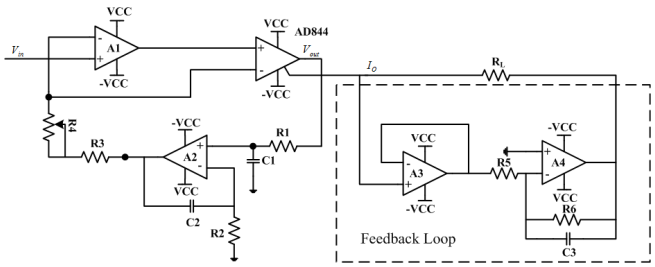

Fig. 4. VCCS with feedback loop

Fig.4 shows voltage controlled current source circuit with feedback loop. A3 and A4 are high speed operational amplifiers. C3 is the capacitor for hindering the free oscillation and stabling the high frequencies performance.

III. Performance Evaluation and Measurement Results

The output sine waveforms are measured by using oscilloscope while the current source drivers a 1kΩ. Fig.5 shows the multiple frequency waveforms which are the sum of three frequencies of 100 KHz, 500 KHz, and 900 KHz in actual measurement by using Agilent Oscilloscope. And initial phases are 0, $\frac{\pi}{3}$ and $\frac{4\pi}{3}$ respectively. From the Fig5, it can be seen that the output sine waveforms in actual measurement are consistent with waveforms in simulation with Modelsim. It shows that the excitation current source can output the multi-frequency, the high stable excitation signals.

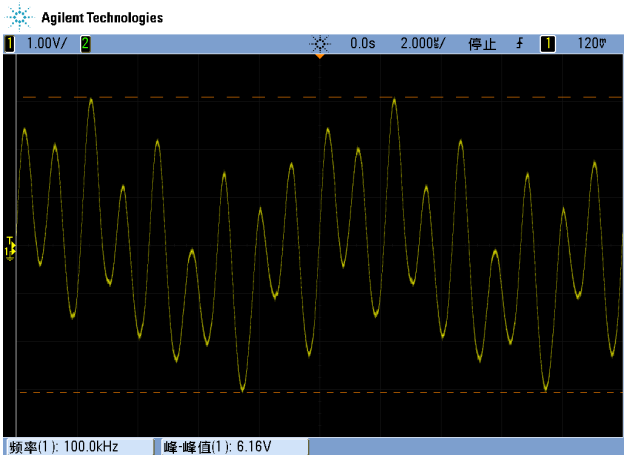

Fig. 5. Multiple frequency waveforms

In order to evaluate the performance of current source, the output impedance is measured. The output impedance can be calculated according to Eq. (4) by changing the load R_L and measure two different load voltages [21].

$$R_O = \left| \frac{R_1 R_2 (U_1 - U_2)}{R_1 U_2 - R_2 U_1} \right| \tag{4}$$

Where U_1 and U_2 are, respectively the output voltages at the load of the R_1 and R_2. R_O is the output impedance.

The simulation of this current source is performed using Multisim 12.0. The output impedance of current source with feedback loop is compared with the current source without feedback loop shown in Fig.6. Fig.6 shows that the output impedance of current source with feedback loop is greater than that of current source without feedback loop. Without feedback loop in VCCS circuits, the output impedance is about 400KΩ at 1MHz and rapidly decreases beyond 100 KHz. With the feedback loop in VCCS circuits, the output impedance is greater than 3.5 MΩ from 1 KHz to 1MHz. It shows that the output impedance is improved by adding feedback loop.

In order to evaluate the stability of current source, the output current of current source is measured for different resistive and capacitive loads by the simulation. The simulation results are shown in Fig.7 and Fig.8. From the Fig.7, it can be seen that output currents of both current sources with and without feedback are constant and steady from 1 KHz to 400 KHz for different loads of 100Ω, 500Ω, 1kΩ and 2kΩ. When the frequency is beyond 400 KHz, maximum variation of current source with feedback loop remains under 0.15%. And maximum variation of current source without feedback loop remains under 0.3%.

For capacitive loads, the Cole-Cole load which represents the electrical equivalent circuit for a biological tissue is adopted in simulation. The Cole-Cole mode is shown in Fig9. In simulation, the resistances of Cole-Cole load are defined to R_i=R_e=2kΩ, and the capacitance varies for C_m=20, 40, 60, 80pF. From the Fig.8, the output current of current source with feedback loop can keep constant in the case of frequency under 100KHz and capacitive load from 20pF to 80pF. When the frequency is below 1 MHz, the output current of current source with feedback loop decreases 0.75%~1.05% at 1 MHz in comparison to 1 kHz. And the output current of current source without feedback loop decreases 1.35%~1.8% at 1 MHz in comparison to 1 kHz. It shows that the stability of current source with feedback loop is better than the current source without feedback loop.

Output impedance of current source with feedback circuit is measured using Agilent Oscilloscope. The two loads are 1kΩ and 2kΩ. In actual measurement, FPGA produces single frequency excitation signals from 1 KHz to 1MHz, which is achieved by changing internal parameters of DDS IP core. The voltages at the loads of 1kΩ and 2kΩ are collected by Agilent Oscilloscope. The output impedance is calculated using Eq. (3). The test result is shown in Fig.10. The output impedance of current source with feedback loop is 1.357 MΩ at 100 KHz and 252kΩ at 1MHz, which can meet requirement of EIT system. It is greater than current source without feedback loop whose output impedance is 1.041 MΩ at 100 KHz and 121kΩ at 1MHz. It shows that output impedance of current source significantly improves by adding feedback loop. It is very meaningful to obtain a further SNR improvement and improve the performance of EIT system.

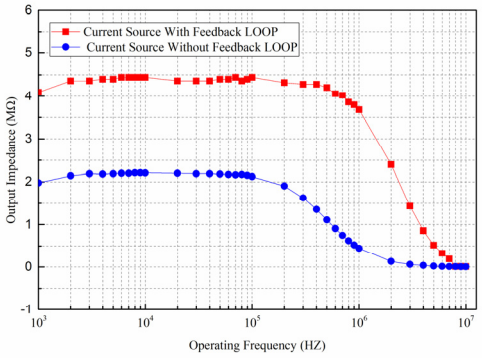

Fig. 6. Comparison of output impedance of both current sources with and without feedback loop in simulation

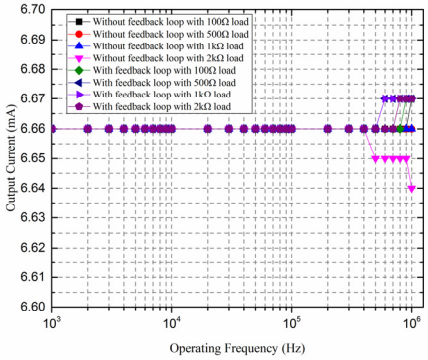

Fig. 7. Comparison of output current of both current sources with and without feedback loop for different resistive loads in simulation

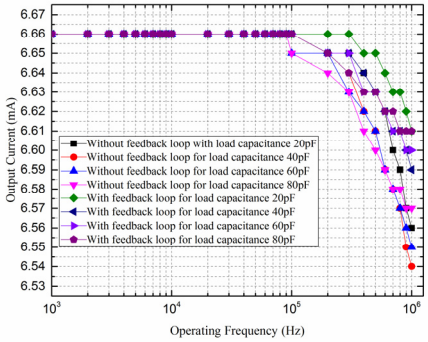

Fig. 8. Comparison of output current of both current sources with and without feedback loop for different capacitive loads in simulation

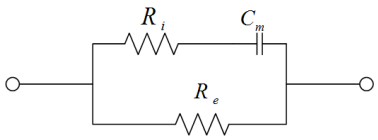

Fig. 9. Cole-Cole model for biological tissue

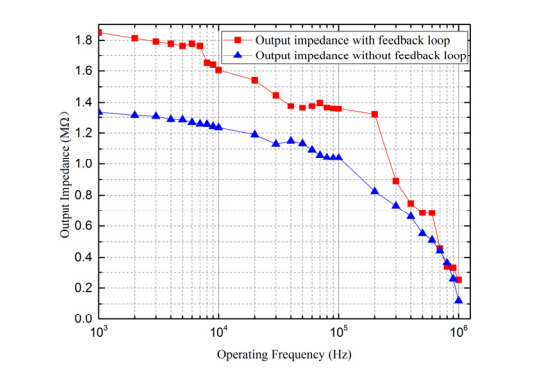

Fig. 10. Comparison of output impedance of both current sources with and without feedback loop in actual measurement

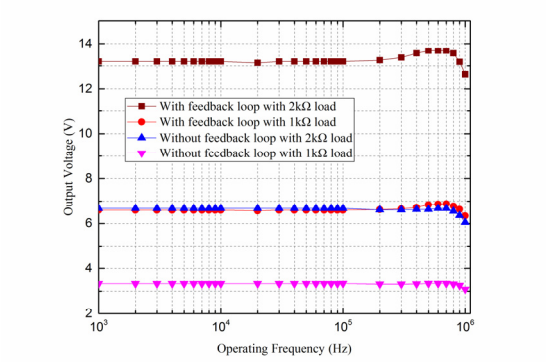

Fig. 11. Output voltage of current source with feedback circuit over the frequency range with different load in actual measurement

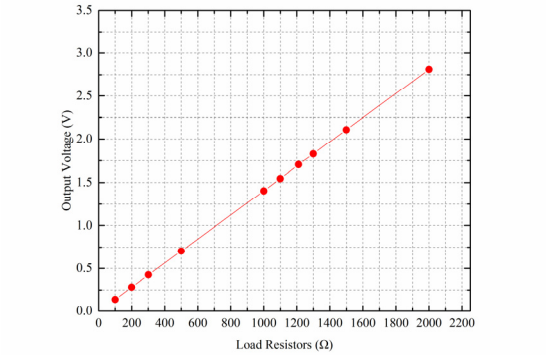

Fig. 12. Output voltage of simultaneous multi-frequency current source with different loads in actual measurement

The amplitude of current source is measured using Agilent Oscilloscope while the current source drivers a 1kΩ and 2kΩ from 1 KHz to 1MHz. The experiment and test results show in Fig.11. From the Fig.11, it can be seen that the amplitudes of output voltages of both current sources with and without feedback loop for the different loads of 1kΩ and 2kΩ are nearly constant below 200 KHz. The amplitudes of output voltage of both current sources are varied with the increase of frequency. The voltages drop rapidly at 1MHz. The output voltage of both current sources at the load of 2kΩ is about twice as the output voltage at the load of 1kΩ. When frequency is below 200 KHz, maximum variation of output current with feedback loop is under 0.5% from 1 KHz to 200 KHz for the different loads of 1kΩ and 2kΩ. Maximum variation of output current without feedback loop is under 0.9% from 1 KHz to 200 KHz for the different loads of 1kΩ and 2kΩ. It shows that both current sources have good performance in low frequency, and the stability of current source with feedback loop is better than the current source without feedback loop in actual measurement. But the output current has relatively large variation at high frequency. The performance of the current source at high frequency with feedback loop is to be improved in the future work.

In order to evaluate the performance of multi-frequency current source, the output voltage with different load is measured using a multimeter. The multiple frequency waveforms are the sum of three frequencies of 10 KHz, 50 KHz and 100 KHz. The experiment and test results show that the output voltage signal of the multi-frequency current source varies linearly with load resistor shown in Fig.12, which illustrates that this simultaneous multi-frequency current source can guarantee constant output current with three-frequency excitation.

IV. CONCLUSIONS

The output impedance and stability of multi-frequency current source are the important factors contributing to improve the precision and sensitivity in multi-frequency electrical impedance tomography system. In this paper, a FPGA-based multi-frequency current source is proposed. FPGA is used to produce the mixture of multiple frequencies, a 14 bit DAC is used to convert the digital sine wave signal into analog voltage signal, the voltage signal is converted to current by using voltage controlled current source (VCCS) circuit based on AD844, and the feedback circuit is specifically designed to improve output impedance. Initial phase of each frequency is controlled to obtain a further SNR improvement by changing internal parameters of DDS IP core.

The output performance is evaluated by simulation and actual measurement. The output impedance of current source with feedback loop is greater than 3.5 MΩ at 1MHz in simulation and 252kΩ at 1MHz in actual measurement, while the output impedance of current source without feedback loop is 446kΩ at 1MHz in simulation and 121kΩ in actual measurement. The output impedance of current source with feedback loop is greater than 1MΩ up to 200 KHz in actual measurement, which is adequate for the most bioelectrical impedance applications. The output performance is measured in this paper. The output voltages of multi-frequency current source follow linearly with different loads with multi-frequency excitation which is sum of 10 KHz, 50 KHz and 100 KHz. It shows that the excitation current source can output the multi-frequency, the high stable excitation signals.

In actual measurement, input signal is produced by FPGA. The different output frequency is performed by changing internal parameters of DDS IP core. It will maybe degrade the output performance of this current source compared with the current source in other designs whose input signal is produced by high precision signal generator. The precision of input signal will still need to be improved in the future work.

Though the simulation and practical measurement, preliminary experimental results demonstrate the feasibility of creating a high precision, multiple-frequency current source for EIT applications.

Some work including simplifying the circuit configuration, reducing the influence of the distribution parameters and the parasitic parameters as well as improving the resolution and precision of the input signal needs to be investigated further to improve the performance of the proposed method in the future.

REFERENCES

[1] G. J. Saulnier, R. S. Blue, J. C. Newell, D. Isaacson, and P. M. Edic, "Electrical impedance tomography," IEEE Signal. Proc. Mag, vol. 18, pp. 31-43, 2001.

[2] S. A. Santos, T. Schlebusch and S. Leonhardt, "Simulation of a Current Source with a Cole-Cole Load for multi-frequency Electrical Impedance Tomography," 35th annual international conference of the ieee engineering in medicine and biology society (embc), pp. 6445-6448, 2013.

[3] A. S. Tucker, R. M. Fox and R. J. Sadleir, "Biocompatible, High Precision, Wideband, Improved Howland Current Source With Lead-Lag Compensation," IEEE T .Biomed. Circ. S, vol. 7, pp. 63-70, 2013.

[4] Sanchez B, Louarroudi E, Jorge E, et al. "A new measuring and identification approach for time-varying bioimpedance using multisine excitation electrical impedance spectroscopy", Physiol Meas, 2013, 34(3): 339-357.

[5] Y. Yang, M. Kang, Y. Lu, J. Wang, J. Yue, and Z. Gao, "Design of a wideband excitation source for fast bioimpedance spectroscopy," Meas. Sci. Technol., vol. 22,013001 (8pp) ,2011.

[6] T. R. Qureshi, C. R. Chatwin, N. Huber, A. Zarafshani, B. Tunstall, and W. Wei, "Comparison of Howland and general impedance converter (GIC) circuit based current sources for bio-impedance measurements," UK, 2010, pp. 012167 (4 pp.).

[7] H. Hongwei, A. Demosthenous, I. F. Triantis, P. Langlois, and R. Bayford, "A high output impedance CMOS current driver for bioimpedance measurements," Piscataway, NJ, USA, 2010, pp. 230-233.

[8] P. Bertemes-Filho, B. H. Brown and A. J. Wilson, "A comparison of modified Howland circuits as current generators with current mirror type circuits," Physiol. Meas., vol. 21, pp. 1-6, 2000.

[9] A. S. Ross, G. J. Saulnier, J. C. Newell, and D. Isaacson, "Current source design for electrical impedance tomography," Physiol. Meas., vol. 24, pp. 509-516, 2003.

[10] H. Wi, H. Sohal, A. L. McEwan, E. J. Woo, and T. I. Oh, "Multi-Frequency Electrical Impedance Tomography System With Automatic Self-Calibration for Long-Term Monitoring," IEEE T .Biomed. Circ. S, vol. 8, pp. 119-128, 2014.

[11] R. Bragos, J. Rosell and P. Riu, "A wide-band AC-coupled current source for electrical impedance tomography," *Physiol Meas,* vol. 15 Suppl 2a, pp. A91-9, 1994-05-01 1994.

[12] J. Kourunen, T. Savolainen, A. Lehikoinen, M. Vauhkonen, and L. M. Heikkinen, "Suitability of a PXI platform for an electrical impedance tomography system," Measurement Science & Technology, vol. 20, 2009.

[13] Y. Yang, L. Wang, P. Wang, X. Yang, F. Zhang, H. Wen, and Z. Teng, "Design of tri-level excitation signals for broadband bioimpedance spectroscopy," *Physiol Meas,* vol. 36, pp. 1995-2007, 2015-09-01 2015.

[14] Y. Yang, F. Zhang, K. Tao, L. Wang, H. Wen, and Z. Teng, "Multi-frequency simultaneous measurement of bioimpedance spectroscopy based on a low crest factor multisine excitation excitation," *Physiol Meas,* vol. 36, pp. 489-501, 2015-03-01 2015.

[15] E. Van der Ouderaa, J. Schoukens and J. Renneboog, "Peak factor minimization of input and output signals of linear systems.," *IEEE Transactions on Instrumentation and Measurement,* vol. 37, pp. 207-212, 1988-01-01 1988.

[16] B. Sanchez, G. Vandersteen, R. Bragos, and J. Schoukens, "Basics of broadband impedance spectroscopy measurements using periodic excitations," Measurement Science & Technology, vol. 23, 2012.

[17] M. R. Schroeder, "Synthesis of low-peak-factor signals and binary sequences with low autocorrelation," *IEEE Transactions on Information Theory,* vol. IT-16, pp. 85-9, 1970-01-01 1970.

[18] Z. Xuehui, W. Huaxiang, C. Shenghua, and Z. Yan, "FPGA-based multi-frequency excitation and modulation technology in EIT system,", Piscataway, NJ, USA, 2010, pp. 907-11.

[19] X. Yue and C. McLeod, "FPGA design and implementation for EIT data acquisition," Physiol. Meas., vol. 29, pp. 1233-1246, 2008.

[20] L. Zhangyong, Z. Xu, C. Ren, W. Wang, D. Zhao, and H. Zhang, "Study of voltage control current source in electrical impedance tomography system," 4th International Conference on Bioinformatics and Biomedical Engineering ,5515066(4pp),2010.

[21] J. Liu, X. Qiao, M. Wang, W. Zhang, G. Li, and L. Lin, "The differential Howland current source with high signal to noise ratio for bioimpedance measurement system," Rev. Sci. Instrum, vol. 85, p. 055111, 20